J. Fluid Mech. (1972), *vol.* 51, *part* 1, *pp.* 137–157
Printed in Great Britain

The unsteady laminar boundary layer on a semi-infinite flat plate due to small fluctuations in the magnitude of the free-stream velocity

By R. C. ACKERBERG AND J. H. PHILLIPS
Polytechnic Institute of Brooklyn Graduate Center, Farmingdale, New York 11735

(Received 20 May 1971)

Asymptotic and numerical solutions of the unsteady boundary-layer equations are obtained for a main stream velocity given by equation (1.1). Far downstream the flow develops into a double boundary layer. The inside layer is a Stokes shear-wave motion, which oscillates with zero mean flow, while the outer layer is a modified Blasius motion, which convects the mean flow downstream. The numerical results indicate that most flow quantities approach their asymptotic values far downstream through damped oscillations. This behaviour is attributed to exponentially small oscillatory eigenfunctions, which account for different initial conditions upstream.

1. Introduction

The study of boundary-layer motions with small periodic fluctuations in the magnitude of the main stream velocity about a steady mean was initiated by Lighthill (1954). He considered the motion past a semi-infinite flat plate with a main stream velocity

$$U = U_0(1 + \epsilon \exp\{i\omega t\}) \quad \text{with} \quad |\epsilon| \ll 1, \tag{1.1}$$

and obtained solutions valid close to and far from the leading edge that were connected using the Kármán–Pohlhausen method. Later work by Rott & Rosenzweig (1960) and Lam & Rott (1960) extended Lighthill's study and investigated the joining of the two solutions by analytical and series methods.

The most interesting feature of this flow develops far downstream, where a double boundary layer may be found. The inside layer is a Stokes shear-wave flow, to first order, and is oscillating with zero mean flow, while a modified Blasius motion exists outside and convects the mean flow downstream. The skin friction anticipates the maxima of the free-stream velocity and its phase is advanced by 45° far downstream.

This paper has two purposes: (i) asymptotic solutions of the boundary-layer equations with the external flow (1.1) are obtained for $\epsilon \to 0$ using the method of matched asymptotic expansions, and (ii) the linear partial differential equation for the perturbation to the steady Blasius flow is solved numerically by a finite-difference method. The work by Lam & Rott (1960) anticipated the use of matched expansions and has many points in common with the work presented

here. However, this is the first systematic presentation that exhibits clearly the asymptotic structure of the solution.

In §2 the problem is formulated mathematically, and it is shown that the appropriate dimensionless streamwise variable is $\xi = \omega x/U_0$, x being the distance from the leading edge. This implies an equivalence of small x with small ω and large x with large ω. Asymptotic solutions for $\xi \to 0$ and $\xi \to \infty$ are obtained in §3, and the limit $\xi \to \infty$ is found to be non-uniform in y, thus requiring a double layer. Composite solutions are derived for $\xi \to \infty$, and it is observed that no freedom (in the choice of constants) exists to account for different initial conditions upstream. This is a result of using only the asymptotic sequence $\{\xi^{-\frac{1}{2}n}\}, n = 0, 1, 2, \ldots$ for $\xi \to \infty$, and a more complete expansion, including exponentially small oscillatory eigensolutions, is proposed in §4. The exponentially small eigenfunctions occur in both layers and are matched in the usual way.

A numerical solution of the partial differential equations describing the first-order perturbation (in ϵ) to the Blasius flow is obtained in §5. A second-order finite-difference method (introduced by Keller & Cebeci 1971), which allows for a variable mesh size across the boundary layer, was used; this technique is especially suited to resolving the double boundary-layer structure.

The numerical results are discussed in §6. A surprising observation is the way in which some quantities approach their asymptotic values far downstream. This does not occur monotonically from below or above, as might be expected, but through damped oscillations about the asymptotic solution. These oscillations are attributed to the exponentially small eigenfunctions and this hypothesis is supported by some numerical results.

2. Mathematical formulation and similarity

Introduce a co-ordinate system with the plate lying along the $\bar{x}$ axis and the $\bar{y}$ axis perpendicular to it and directed into the fluid (see figure 1). Dimensional variables, denoted by bars, are non-dimensionalized as follows:

$$\left.\begin{aligned} t = \omega\bar{t}, \quad x = \omega\bar{x}/U_0, \quad y = (\omega/\nu)^{\frac{1}{2}}\bar{y}, \quad \psi(x,y,t) = (\omega/\nu U_0^2)^{\frac{1}{2}}\bar{\psi}(\bar{x},\bar{y},\bar{t}), \\ u = \bar{u}/U_0 = \psi_y, \quad v = (\omega\nu)^{-\frac{1}{2}}\bar{v} = -\psi_x. \end{aligned}\right\} \tag{2.1}$$

Here ω is the frequency of the perturbation to the free stream, which has mean velocity U_0, ν is the kinematic viscosity, ψ is the stream function, (u, v) are the velocity components in the (x, y) directions, and alphabetic subscripts denote partial differentiation, It is assumed that the boundary-layer equations are valid for all $x > 0$, although it is known that they fail in a small neighbourhood of the leading edge, where the Navier–Stokes equations must be used. In terms of the stream function, the x-momentum equation can be written

$$\psi_{yt} + \psi_y\psi_{yx} - \psi_x\psi_{yy} = U_t + \psi_{yyy}, \tag{2.2}$$

where $U(t)$, the non-dimensional x component of velocity just outside the boundary layer, is given by

$$U(t) \equiv 1 + \epsilon \exp\{it\}, \tag{2.3}$$

and ϵ is a dimensionless parameter (see (1.1)).

The no-slip requirement at the plate and the asymptotic condition at the edge of the boundary layer will be satisfied if

$$\psi_y(x,0,t) = 0 = \psi(x,0,t) \quad \text{for} \quad x > 0, \tag{2.4}$$

and

$$\psi_y(x,y,t) \to U(t) \quad \text{for} \quad y \to \infty. \tag{2.5}$$

An initial condition at the leading edge requires

$$\psi_y(0,y,t) = H(y,t) \quad \text{for} \quad y,t > 0. \tag{2.6}$$

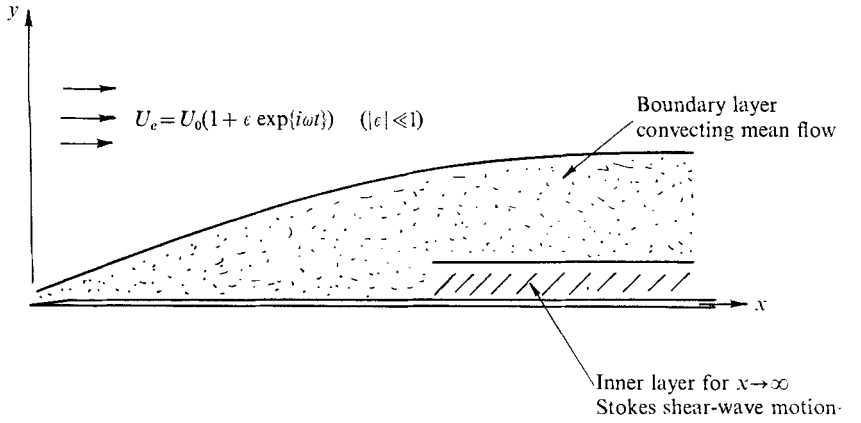

FIGURE 1. Flow geometry.

In this paper, H will be independent of y and correspond to the velocity in the main stream. Finally, a periodicity condition requires

$$P(x,y,t) = P(x,y,t+T), \tag{2.7}$$

where P is any property of the flow field (e.g. velocity), and the non-dimensional period $T = 2\pi$. It is expected that the periodic solutions sought here may be obtained as limiting solutions ($t \to \infty$) of appropriate initial-value problems.

2.1. *Similarity*

From (2.2)–(2.6) it is clear that if a solution exists, it must have the functional form

$$\bar{\psi}(\bar{x},\bar{y},\bar{t}) = (\nu/\omega)^{\frac{1}{2}} U_0 \mathscr{F}[\omega\bar{x}/U_0, (\omega/\nu)^{\frac{1}{2}}\bar{y}, \omega\bar{t}; \epsilon]. \tag{2.8}$$

Note that ϵ has not yet been assumed small; however, it cannot be so large as to invalidate the use of boundary-layer theory, e.g. back flow near the leading edge must not occur. Also, additional parameters may be introduced in (2.8) through the boundary and initial conditions.

The form of this solution suggests an equivalence (or similarity) of small ω with small x and large ω with large x; this provides the motivation for seeking a quasi-steady solution ($\omega \to 0$) when x is small and a Stokes shear-wave motion ($\omega \to \infty$) far downstream. However, the limit $x \to \infty$ is not uniform in y, and a double boundary layer will be required.†

† It should be observed that Lin's (1956) result for $\omega \to \infty$ with ϵ unrestricted also follows from this similarity.

2.2. *Small parameter expansion*

We seek an asymptotic solution $\epsilon \to 0$ which is valid for all (x, y). When $\epsilon \equiv 0$, the problem reduces to steady uniform flow past a semi-infinite flat plate and the solution, with uniform flow at the leading edge, has been given by Blasius. Although ω appears in the non-dimensionalization (2.1) for this limiting case, it will not appear when the Blasius solution,

$$\psi_0(x, y) = (2x)^{\frac{1}{2}} F(\eta) \quad \text{where} \quad \eta = y/(2x)^{\frac{1}{2}}, \tag{2.9}$$

is written in dimensional form. Here F is a solution of

$$F''' + FF'' = 0, \tag{2.10}$$

subject to

$$F(0) = 0 = F'(0), \tag{2.11}$$

and

$$F'(\eta) \to 1 \quad \text{for} \quad \eta \to \infty.\dagger \tag{2.12}$$

Since this solution satisfies (2.2)–(2.6) when $\epsilon = 0$, it is taken to be a uniformly valid first approximation.

To obtain higher order terms we require $|\epsilon| \gg \omega\nu/U_0^2$. The parameter $U_0^2/\omega\nu$ plays the role of a conventional Reynolds number, and the inequality guarantees that the predominant perturbation to the Blasius flow is the free-stream fluctuation and not a higher order correction to boundary-layer theory. It is convenient to introduce new independent variables (x, η, t) so the boundary-layer thickness, in terms of η, will be nearly constant; this is a consequence of the mean flow being convected by the Blasius motion while the perturbation does not produce any net flux far downstream. Since this transformation is not one-one at $x = 0$, where any $y \geqslant 0$ is mapped onto $\eta = \infty$, (2.6) cannot be satisfied in a general way. However, this limitation is not very restrictive physically, since the point of attachment of the undisturbed stream is usually at the leading edge. In special cases, the original variables would be more appropriate.

Transforming (2.2) to the variables $(\xi = x, \eta = y/(2x)^{\frac{1}{2}}, t)$‡ and writing

$$\psi(x, y, t) = (2\xi)^{\frac{1}{2}} \Phi(\xi, \eta, t), \tag{2.13}$$

with

$$u = \Phi_\eta \quad \text{and} \quad v = (2\xi)^{-\frac{1}{2}} [\eta\Phi_\eta - 2\xi\Phi_\xi - \Phi], \tag{2.14}$$

we obtain an equation for Φ, i.e.

$$\Phi_{\eta\eta\eta} + \Phi\Phi_{\eta\eta} - 2\xi[\Phi_{\eta t} + \Phi_\eta \Phi_{\eta\xi} - \Phi_{\eta\eta}\Phi_\xi - \epsilon i \exp\{it\}] = 0. \tag{2.15}$$

In (2.15) we have used (2.3). Since the resulting equations for the perturbations will be linear, we assume, without loss of generality,

$$\Phi(\xi, \eta, t) = F(\eta) + \epsilon \exp\{it\} G(\xi, \eta). \S \tag{2.16}$$

Substituting in (2.15), we find, after equating to zero the coefficient of ϵ,

$$G_{\eta\eta\eta} + FG_{\eta\eta} + F''G - 2\xi[iG_\eta + F'G_{\eta\xi} - F''G_\xi - i] = 0. \tag{2.17}$$

† Primes denote differentiation with respect to η and $F''(0) = 0{\cdot}4696$.

‡ This definition of ξ differs from that of Lam & Rott (1960) by a factor of i.

§ There are steady perturbation solutions of (2.15) with the form

$$\phi(\xi, \eta) = F(\eta) + \epsilon\xi^k S_k(\eta),$$

where $S_k(\eta)$ are the eigensolutions discussed by Libby & Fox (1963) and $k < 0$. These are not finite at the leading edge, and are rejected.

The boundary conditions (2.4) and (2.5) require

$$G_\eta(\xi, 0) = 0 = G(\xi, 0), \tag{2.18}$$

and

$$G_\eta(\xi, \eta) \to 1 \quad \text{for} \quad \eta \to \infty. \tag{2.19}$$

The initial condition at the leading edge will be satisfied if G is a solution of (2.17) with $\xi \equiv 0$, satisfying (2.18) and (2.19); this solution is

$$G(0, \eta) = \tfrac{1}{2}(\eta F' + F), \tag{2.20}$$

and it can be identified as the quasi-steady solution given by Lighthill (1954) (see his equation (7)).

An important question should now be asked: Will the solution of (2.17)–(2.20) be uniformly valid in space when $\epsilon \to 0$? As we shall see in the following sections, the answer seems to be in the affirmative (neglecting the leading edge), because the asymptotic *coordinate* expansions of (2.17) exhibit the structure expected from the similarity (2.8), and all boundary and initial conditions can be satisfied.

3. Asymptotic solutions

3.1. *Expansion for small x*

An asymptotic expansion for $\xi \to 0$ has been obtained by Rott & Rosenzweig (1960) and Lam & Rott (1960). It has the form

$$G(\xi, \eta) \sim \sum_{n=0} (2i\xi)^n h_n(\eta), \dagger \tag{3.1}$$

where h_n satisfies

$$h_n''' + F h_n'' - 2nF' h_n' + (1 + 2n) F'' h_n = \mathscr{H}_n(h_{n-1}'), \tag{3.2}$$

subject to the conditions

$$h_n(0) = 0 = h_n'(0) \quad \text{for} \quad n \geqslant 0, \tag{3.3}$$

and

$$h_0'(\infty) = 1, \quad h_n'(\infty) = 0 \quad \text{for} \quad n \geqslant 1. \tag{3.4}$$

Here $\mathscr{H}_0 = 0$, $\mathscr{H}_1 = h_0' - 1$, and $\mathscr{H}_{n+1} = h_n'$ for $n \geqslant 1$. It should be noted that the homogeneous equation (3.2) subject to homogeneous boundary conditions has eigensolutions only for $n < 0$, and these are physically inadmissible owing to the singularity at $\xi = 0$.‡

The function $h_0(\eta)$ is identical with (2.20) and 15 additional terms were computed numerically by Lam & Rott (1960, p. 15), who tabulated the values $h_n''(0)$ $(n = 0, 1, \ldots, 15)$. Values of $\tau_w(\xi) = G_{\eta\eta}(\xi, 0)$ were computed and the resulting curves are shown in figure 4 as the dashed lines. The results are in excellent agreement with the numerical solutions for $\xi \leqslant 1{\cdot}5$.

† In the referenced papers, $h_n(\eta)$ is denoted by $g_n(\eta)$.

‡ It has been assumed that (2.17) is valid at $x \equiv 0$; in fact, we can only require the boundary-layer solution to match with a solution of the Navier–Stokes equations, valid near $x = 0$. Thus, the singular eigensolutions should not be rejected so readily. However, they would not appear in any numerical solution of (2.17), since the skin friction $G_{\eta\eta}$ would not be integrable with respect to x.

3.2. *Expansions for large x*

This expansion is obtained by introducing the new independent variable,

$$\alpha = \xi^{-\frac{1}{2}}, \tag{3.5}$$

in place of ξ. Equation (2.17) becomes

$$2i(G_\eta - 1) - \alpha^2(G_{\eta\eta\eta} + FG_{\eta\eta} + F''G) + \alpha^3(F''G_\alpha - F'G_{\eta\alpha}) = 0, \tag{3.6}$$

subject to the same boundary conditions (2.18)–(2.19).

We formally let $\alpha \to 0$ in (3.6), keeping η fixed, and obtain

$$G^0_\eta - 1 = 0, \tag{3.7}$$

which has solution, $$G^0(\eta) = \eta + C_0.$$

Clearly both boundary conditions (2.18) cannot be satisfied, and a slip velocity will occur at $\eta = 0$. This suggests a non-uniform limit which may be removed using an 'inner expansion'. We assume G^0 represents the first term of an 'outer expansion' since it satisfies (2.19).

The appearance of a double layer owing to the co-ordinate expansion $\alpha \to 0$ is not unusual and is common in problems of boundary-layer separation (see Goldstein 1930; Ackerberg 1970). To put these situations in the framework of matched asymptotic expansions with a small parameter, an artificial parameter can be introduced or the co-ordinate undergoing the limit process may be considered a small or large parameter.

3.3. *Outer expansion*

The appearance of algebraic powers of α in (3.6) suggests an expansion of the form

$$G(\alpha, \eta) \sim \sum_{n=0} \alpha^n \bar{G}_n(\eta) \quad \text{for} \quad \alpha \to 0, \quad \eta = O(1). \tag{3.8}$$

Substituting in (3.6), we find equations for the $\bar{G}_n$'s:

$$\bar{G}_0' = 1, \quad \bar{G}_1' = 0, \quad i\bar{G}_2' = \tfrac{1}{2}F''\bar{G}_0, \tag{3.9}$$

$$i\bar{G}_{n+3}' = \tfrac{1}{2}(\bar{G}_{n+1}''' + F\bar{G}_{n+1}'') + \tfrac{1}{2}(n+1)F'\bar{G}_{n+1}' - (\tfrac{1}{2}n)F''\bar{G}_{n+1} \quad \text{for} \quad n \geqslant 0, \tag{3.10}$$

which are subject to the outer boundary conditions

$$\bar{G}_0' \to 1 \quad \text{and} \quad \bar{G}_n' \to 0 \quad (n > 0) \quad \text{for} \quad \eta \to \infty. \tag{3.11}$$

The solutions are

$$\bar{G}_0 = \eta + C_0, \quad \bar{G}_1 = C_1, \quad \bar{G}_2 = (2i)^{-1}(\eta F' - F + C_0 F'), \tag{3.12}$$

$$\bar{G}_3 = C_3, \quad \bar{G}_4 = C_4, \quad \bar{G}_5 = C_5, \tag{3.13}$$

and, using mathematical induction,

$$\bar{G}_{n+1} = (2i)^{-1}(2-n)C_{n-1}F' + C_{n+1} \quad \text{for} \quad n \geqslant 5. \tag{3.14}$$

The unknown constants C_n will be determined by the matching procedure to be discussed later.

3.4. *Inner expansion*

Introduce the independent and dependent variables

$$\alpha = \xi^{-\frac{1}{2}}, \quad \sigma = (2\xi)^{\frac{1}{2}}\eta \equiv y, \quad g(\alpha,\sigma) = (2\xi)^{\frac{1}{2}}G(\xi,\eta). \tag{3.15}$$

Transforming (2.17), we find

$$4g_{\sigma\sigma\sigma} + 2^{\frac{3}{2}}\alpha F g_{\sigma\sigma} - 4ig_\sigma - 2\alpha^2 F'(\sigma g_{\sigma\sigma} - \alpha g_{\sigma\alpha}) + 2^{\frac{1}{2}}\alpha^3 F''(\sigma g_\sigma - \alpha g_\alpha) + 4i = 0. \tag{3.16}$$

In these coordinates, the velocity components may be written

$$u = F' + \epsilon \exp\{it\} g_\sigma \quad \text{and} \quad v = 2^{-\frac{1}{2}}\alpha(\eta F' - F) + 2^{-1}\epsilon \exp\{it\}\alpha^3 g_\alpha. \tag{3.17}$$

The outer solution was obtained as the limit $\alpha \to 0$ with η fixed, but here we let $\alpha \to 0$ with σ fixed. Therefore, the coefficients in (3.16), which are functions of $\eta (= 2^{-\frac{1}{2}}\alpha\sigma)$, should be expanded for $\eta \to 0$ and rewritten in terms of (α, σ). Noting

$$F(\eta) = C\eta^2 + O(\eta^5) \quad \text{with} \quad C = 0{\cdot}2348\ldots,$$

(3.16) can be written

$$4g_{\sigma\sigma\sigma} + 2^{\frac{1}{2}}C\sigma^2\alpha^3 g_{\sigma\sigma} - 4ig_\sigma + 2^{\frac{3}{2}}C[\sigma\alpha^3(\alpha g_{\sigma\alpha} - \sigma g_{\sigma\sigma}) + \alpha^3(\sigma g_\sigma - \alpha g_\alpha)] + 4i + O(\alpha^6) = 0. \tag{3.18}$$

The no-slip condition will be satisfied if

$$g(\alpha, 0) = 0 = g_\sigma(\alpha, 0). \tag{3.19}$$

Assume

$$g(\alpha,\sigma) \sim \sum_{n=0} \alpha^n g_n(\sigma) \quad \text{for} \quad \alpha \to 0, \quad \sigma = O(1), \tag{3.20}$$

and substitute (3.20) in (3.18). We find the following differential equations for the g_n's:

$$g_0''' - ig_0' + i = 0, \tag{3.21}$$

$$g_1''' - ig_1' = 0, \tag{3.22}$$

$$g_2''' - ig_2' = 0, \tag{3.23}$$

$$g_3''' - ig_3' - 2^{-\frac{3}{2}}C(\sigma^2 g_0'' - 2\sigma g_0') = 0, \tag{3.24}$$

$$g_4''' - ig_4' = 0, \tag{3.25}$$

$$g_5''' - ig_5' = 0. \tag{3.26}$$

Here primes denote differentiation with respect to σ. The solutions, subject to (3.19), are

$$g_0(\sigma) = \sigma + s^{-1}(\exp\{-s\sigma\} - 1), \tag{3.27}$$

$$g_1(\sigma) = 0 = g_2(\sigma), \tag{3.28}$$

$$g_3(\sigma) = 2^{-\frac{3}{2}}C\{\tfrac{1}{4}(1 - \exp\{-s\sigma\}) - i\sigma^2 + \exp\{-s\sigma\}[(6s)^{-1}\sigma^3 - (5i\sigma^2/4) - (13s\sigma/4)]\}, \tag{3.29}$$

$$g_4(\sigma) = 0 = g_5(\sigma), \tag{3.30}$$

where $s = \sqrt{i}$, and g_0 is the Stokes shear-wave solution for an infinite flat plate in an oscillating free stream with zero mean flow.

3.5. *Matching*

Although each term in the inner expansion is completely determined, unknown constants are introduced in the outer expansion at each order. They are determined by the following matching principle:

$$\lim_{\sigma\to\infty} G^i(\alpha,\sigma) = \lim_{\eta\to 0} G^o(\alpha,\eta).\dagger \tag{3.31}$$

Carrying out the limit on the left using (3.15), (3.20) and (3.27)–(3.30), neglecting exponentially small terms, we obtain

$$G^i(\alpha,\sigma) \sim 2^{-\frac{1}{2}}\alpha\{\sigma - s^{-1} + 2^{-\frac{3}{2}}C\alpha^3(\tfrac{13}{4} - i\sigma^2) + O(\alpha^6)\} \tag{3.32a}$$

$$\sim \eta - \alpha(2^{-\frac{1}{2}}s^{-1}) - \alpha^2(\tfrac{1}{2}iC\eta^2) + (\tfrac{13}{16})C\alpha^4 + O(\alpha^7). \tag{3.32b}$$

In (3.32*b*), we have written the result in terms of (α,η). The terms of $O(\alpha^7)$ in (3.32*a*), when written in terms of (α,η) will not contribute to any of the terms already appearing in (3.32*b*), although additional terms of the form $\alpha^7, \alpha^2\eta^5$, $\alpha^6\eta$, etc. might arise.

We now expand the outer solution given by (3.8), (3.12)–(3.14) for $\eta \to 0$ to obtain

$$G^o(\alpha,\eta) \sim \eta + C_0 + \alpha C_1 + (\alpha^2/2i)\,[C\eta^2 + 2CC_0\eta + O(\eta^4)] + \alpha^3 C_3 + \alpha^4 C_4 + \alpha^5 C_5 + \alpha^6[3iCC_4\eta + C_6 + O(\eta^4)] + O(\alpha^7). \tag{3.33}$$

For each term in (3.32*b*) there should be a corresponding term in (3.33). This can be achieved by choosing the unknown constants in the following way:

$$C_0 = 0, \quad C_1 = -2^{-\frac{1}{2}}s^{-1}, \quad C_3 = 0, \quad C_4 = \tfrac{13}{16}C, \quad C_5 = 0 = C_6. \tag{3.34}$$

We observe that the non-zero term of $O(\alpha^6\eta)$ in (3.33) would arise from a term of $O(\alpha^7)$ in (3.32*a*), and there is no inconsistency.

3.6. *Summary and composite solutions for* $x \to \infty$

The inner and outer expansions may be written

$$G^i(\alpha,\sigma) \sim 2^{-\frac{1}{2}}\alpha[g_0(\sigma) + \alpha^3 g_3(\sigma) + O(\alpha^6)] \quad \text{for} \quad \alpha \to 0, \quad \sigma = O(1), \tag{3.35}$$

$$G^o(\alpha,\eta) \sim \eta - \alpha(2^{-\frac{1}{2}}s^{-1}) + (\alpha^2/2i)\,(\eta F' - F) + \tfrac{13}{16}\alpha^4 C + \alpha^6(39i/32)\,CF' + O(\alpha^7) \quad \text{for} \quad \alpha \to 0, \quad \eta = O(1), \tag{3.36}$$

where $g_3(\sigma)$ is given by (3.29) and $F(\eta)$ is the Blasius function.

Using (3.35) and (3.36) we may write a composite solution for the x component of velocity (see Cole 1968, p. 13), i.e.

$$u \sim 1 - \exp\{-s\sigma\} + (\alpha^2/2i)\,\eta F''(\eta) + \alpha^3(2^{-\frac{3}{2}}C)\exp\{-s\sigma\}\,[(3i/4)\sigma - (3/4s)\sigma^2 - \sigma^3/6] + O(\alpha^6) \quad \text{for} \quad \alpha \to 0. \tag{3.37}$$

The skin friction and reduced volumetric flux are

$$\tau(\alpha) = G_{\eta\eta}(\alpha,0) \sim 2^{\frac{1}{2}}s/\alpha - \tfrac{5}{8}i\alpha^2 + O(\alpha^5), \tag{3.38}$$

and

$$R_f = (2x)^{\frac{1}{2}}\int_0^\infty (1 - G_\eta)\,d\eta = 2^{\frac{1}{2}}\alpha^{-1}\lim_{\eta\to\infty}[\eta - G^o(\alpha,\eta)]$$

$$\sim s^{-1} - (2^{\frac{1}{2}}i)^{-1}\alpha\beta - 2^{\frac{1}{2}}(\tfrac{13}{16})\,C\alpha^3 - (\tfrac{39}{32})\,iC\alpha^5 + O(\alpha^6), \tag{3.39}$$

where $\beta = \lim_{\eta\to\infty}(\eta F' - F) = 1{\cdot}21678$.

† The superscripts i and o distinguish the 'inner' and 'outer' expansions, respectively.

4. Eigenfunctions for $x \to \infty$

There would be no difficulty in continuing the asymptotic expansions for large x to higher orders. It is surprising that these expansions are completely determined and independent of the initial conditions upstream that are required to solve a parabolic partial differential equation such as (2.17). The difficulty is that the asymptotic expansions obtained so far are incomplete, for they contain only terms of the asymptotic sequence $\{\alpha^n\}$. In addition, there are a countable number of exponentially small eigensolutions, valid for $x \to \infty$, which can account for different initial conditions in x. A similar situation arises with the boundary-layer flow of a thin film along a vertical plate (see Ackerberg 1968, p. 1287). For that case, an asymptotic shear flow evolves far downstream and is independent of the streamwise co-ordinate; it can be shown that initial conditions decay exponentially fast via the eigenfunctions. It is usually assumed that when algebraically and exponentially small terms occur together, the exponential parts may be neglected insofar as numerical results are concerned. Our study will show this to be false.

The exponentially small eigenfunctions were first found by Lam & Rott (1960). The analysis presented here emphasizes the use of matched asymptotic expansions, and discusses the properties of these solutions.

4.1. *Inner solution*

The first-order term in the inner expansion, for $x \to \infty$ (see (3.20)) is independent of x, the time-like variable. To obtain information about the decay of initial conditions, we retain the largest σ and α derivatives in (3.18) when $\alpha \to 0$, and find

$$4g_{\sigma\sigma\sigma} - 4ig_\sigma + 2^{\frac{3}{2}}C\alpha^4(\sigma g_{\sigma\alpha} - g_\alpha) = 0. \tag{4.1}$$

The particular solution of (3.18), corresponding to the forcing term $4i$, is $g = \sigma$, which is a member of the sequence $\{\alpha^n\}$; thus, if there are exponentially small eigensolutions they will satisfy homogeneous equations.

Assume (4.1) has a solution of the form

$$g(\sigma, \alpha) = A(\alpha)\, S(\sigma). \tag{4.2}$$

After substituting in (4.1) and using separation of variables, we find

$$dA/d\alpha - (\lambda^2/k^2\alpha^4)\, A = 0, \tag{4.3}$$

and

$$d^3S/d\sigma^3 - id S/d\sigma + \lambda^2(\sigma\, dS/d\sigma - S) = 0. \tag{4.4}$$

Here $k^2 = 2^{-\frac{1}{2}}C$ and λ^2 is the separation constant. The solution to (4.3) is

$$A(\alpha) = D \exp\{-\lambda^2(3k^2\alpha^3)^{-1}\}, \tag{4.5}$$

where D is a constant of integration. The solution of (4.4) can be found by differentiating it once with respect to σ, and then putting $w(\sigma) = d^2S/d\sigma^2$, i.e.

$$d^2w/d\sigma^2 + (\lambda^2\sigma - i)\, w = 0. \tag{4.6}$$

The boundary conditions at $\sigma = 0$ requiring $S = 0 = dS/d\sigma$ will be satisfied if

$$dw/d\sigma = 0 \quad \text{at} \quad \sigma = 0, \tag{4.7}$$

and

$$S(\sigma) = \int_0^\sigma (\sigma - t)\, w(t)\, dt. \tag{4.8}$$

A matching condition, to be discussed later, will require that for $\sigma \to \infty$, $S(\sigma)$ must not grow faster than a linear function of σ. This will be satisfied if

$$|S'(\infty)| = \left| \int_0^\infty w(\sigma)\, d\sigma \right| < \infty \quad \text{and} \quad \left| \int_0^\infty \sigma w(\sigma)\, d\sigma \right| < \infty. \tag{4.9}$$

To solve (4.6) subject to (4.7), introduce the new independent variable

$$z = (i - \lambda^2 \sigma) \exp\{i\beta\}/\lambda^{\frac{4}{3}}, \tag{4.10}$$

wnere $\beta = 0, \pm \frac{2}{3}\pi$. Only one solution is obtained for the two values $\beta = \pm \frac{2}{3}\pi$, and to simplify the discussion later we will consider $\beta = 0, -\frac{2}{3}\pi$. Transforming (4.6) and (4.7), we find

$$d^2w/dz^2 - zw = 0, \tag{4.11}$$

with

$$dw/dz = 0 \quad \text{at} \quad z = \mathrm{i} \exp\{i\beta\}/\lambda^{\frac{4}{3}}. \tag{4.12}$$

We recognize (4.11) as Airy's equation, which has two independent solutions, Ai (z) and Bi (z). The function Bi (z) is exponentially large for $|z| \to \infty$ for all values of $\arg z$ except $\arg z = \frac{1}{3}\pi, \pi$, when it is oscillatory and decaying algebraically. If Bi (z) is included in the solution for $w(z)$, it will not be possible to satisfy (4.9) when $\arg z \neq \frac{1}{3}\pi, \pi$. The latter cases may also be excluded from consideration by the matching, for it would require a $G_{\eta\eta}$ from the outer solution which is algebraically large and oscillatory when $\eta \to 0$, and the governing linear partial differential equation would have to exhibit a singular point (or singular forcing term) at $\eta = 0$. This is not the case, and therefore we take

$$w(z) \propto \mathrm{Ai}\,(z). \tag{4.13}$$

We may satisfy (4.12) if

$$(d/dz)\,\mathrm{Ai}\,(z) = 0 \quad \text{when} \quad z = \mathrm{i} \exp\{i\beta\}/\lambda^{\frac{4}{3}}. \tag{4.14}$$

The zeros of the derivative of the Airy function lie along the negative real axis, say at

$$z_i = \rho_i \exp\{\pi i\} \quad (\rho_i > 0,\ \mathrm{i} = 1, 2, \ldots \infty). \tag{4.15}$$

(Values of ρ_i are given in Abramowitz & Stegun (1964, p. 478).) Hence the eigenvalues λ_i must be chosen so that

$$\lambda_i = \rho_i^{-\frac{3}{4}} \exp\{\tfrac{3}{4}i(\beta - \tfrac{1}{2}\pi)\}. \tag{4.16}$$

The eigensolution is then found by determining the range of z corresponding to real values of $\sigma \in [0, \infty)$ from (4.10) with $\lambda = \lambda_i$. Using these values, $w(z)$ and thus $S(\sigma)$ may be determined from (4.13), (4.10) and (4.8).

It is known that Ai (z) tends to zero exponentially fast for $|z| \to \infty$ when $\arg z_\infty \in (-\frac{1}{3}\pi, \frac{1}{3}\pi)$. Outside this range it is exponentially large except for $\arg z = \pi, \pm \frac{1}{3}\pi$, when it is oscillatory and decaying algebraically. The arguments

used for Bi(z) apply here as well, and we must take care that for $\sigma \to \infty$, (4.10) yields a corresponding $\arg z_\infty \in (-\frac{1}{3}\pi, \frac{1}{3}\pi)$. When $\beta = 0$, $\arg z_\infty = \frac{3}{4}\pi$ and for $\beta = -\frac{2}{3}\pi$, $\arg z_\infty = -\frac{1}{4}\pi$. Thus, we choose $\beta = -\frac{2}{3}\pi$, and the eigensolutions satisfying (4.6)–(4.9) may be uniquely determined.

From (4.5) and (4.16), an expression may be found for the streamwise attenuation; it is

$$A_k(\alpha) \propto \exp(-b_k)\begin{cases}\cos b_k \\ \sin b_k\end{cases} \quad (k = 1, 2, 3, \ldots), \tag{4.17}$$

where $b_k = (3C\rho_k^{\frac{3}{2}}\alpha^3)^{-1}$. Since $\rho_k \to \infty$ for $k \to \infty$, it is clear that, for large values of ρ_k, the attenuation may be negligible for moderate and small values of α.

4.2. *Outer solution and matching*

It was observed by Lam & Rott (1960) that a complementary solution of (2.17) is

$$G_c(\xi, \eta) = p(\xi) + (2\xi i)^{-1}[2\xi p_\xi + p(\xi)]F'(\eta), \tag{4.18}$$

where $p(\xi)$ is any differentiable function. We note that $dG_c/d\eta$ satisfies a homogeneous outer boundary condition for $\eta \to \infty$, and we may therefore consider it an eigensolution for the outer flow.

The unknown function $p(\xi)$ can be determined by matching in the following way. We first express p in terms of $\alpha = \xi^{-\frac{1}{2}}$, expand (4.18) for $\eta \to 0$, and write the result in terms of (α, σ), i.e.

$$\begin{aligned} G_c(\alpha, \eta) &= p(\alpha) + (\alpha^2/2i)(p - \alpha p_\alpha)[2C\eta + O(\eta^4)] \\ &= p(\alpha) + (\alpha^2/2i)(p - \alpha p_\alpha)[2^{\frac{1}{2}}C\alpha\sigma + O(\alpha^4\sigma^4)]. \end{aligned} \tag{4.19}$$

From the inner expansion (see (3.15) and (4.2)), we find, for $\sigma \to \infty$,

$$\begin{aligned} G^i(\alpha, \sigma) = 2^{-\frac{1}{2}}\alpha g(\alpha, \sigma) &= 2^{-\frac{1}{2}}\alpha A(\alpha) S(\sigma) \\ &\sim 2^{-\frac{1}{2}}D\alpha \exp\{-\lambda^2(3k^2\alpha^3)^{-1}\}[S_\infty + \sigma S'_\infty], \end{aligned} \tag{4.20}$$

where

$$S'_\infty = \int_0^\infty w(\sigma)\, d\sigma, \quad S_\infty = \lim_{\sigma \to \infty}[S(\sigma) - \sigma S'_\infty] = -\int_0^\infty \sigma w(\sigma)\, d\sigma,$$

and λ is an eigenvalue. Comparing (4.19) and (4.20), we can match the term of $O(\sigma)$ by choosing

$$\alpha p_\alpha - p = -(iDS'_\infty/C\alpha^2)\exp\{-\lambda^2(3k^2\alpha^3)^{-1}\}. \tag{4.21}$$

A peculiar solution of (4.21) is

$$p(\alpha) = -(iDS'_\infty k^2/C\lambda^2)\alpha \exp\{-\lambda^2(3k^2\alpha^3)^{-1}\}. \tag{4.22}$$

The complementary solution $p = \alpha$ is a member of the sequence $\{\alpha^n\}$ and should be discarded. Since a multiple of $p(\alpha)$ is what appears as a multiplicative factor in (4.20), we may further match the term of $O(\sigma^0)$ in (4.19) and (4.20) to obtain the relation,

$$S_\infty/S'_\infty = -i/\lambda^2. \tag{4.23}$$

This equation can be verified by integrating (4.6) over the range $[0, \infty)$ and noting $w'(0) = 0$; thus the matching is self-consistent. We note that each eigenfunction

will generate offspring owing to the neglected terms in deriving (4.1) from (3.18). The members of each family will match with the additional terms in (4.19). We shall find that the exponentially small eigensolutions are important for interpreting the numerical results of § 5.

5. Numerical solution by finite-difference methods

Since the solution of (2.17), for large x, involves a double layer, a numerical method is chosen which allows for variable mesh spacing in the y direction to achieve better resolution inside the boundary layer. Keller & Cebeci (1971) have proposed a second-order implicit technique with this feature, and it will be used here with a modification.

To apply this method, we first write (2.17) as a first-order system with dependent variables $G(\xi,\eta)$, $w(\xi,\eta)$, $z(\xi,\eta)$, i.e.

$$G_\eta = w, \tag{5.1}$$

$$w_\eta = z, \tag{5.2}$$

$$z_\eta = -Fz - F''G + 2\xi[F'w_\xi - F''G_\xi + i(w-1)]. \tag{5.3}$$

We introduce the mesh points (ξ_j,η_m) for $\xi \geqslant 0$, $0 \leqslant \eta \leqslant \eta_\infty$, and use the notation

$$\xi_1 = 0; \quad \xi_j = \xi_{j-1} + k_{j-1} \quad (j = 2,3,\ldots), \tag{5.4}$$

$$\eta_1 = 0, \quad \eta_m = \eta_{m-1} + h_{m-1}, \quad m = 2,3,\ldots,M \quad \text{and} \quad \eta_M = \eta_\infty. \tag{5.5}$$

Here k_j and h_m are variable mesh widths. Centred differences are used throughout and we approximate (5.1) and (5.2) at the point $(\xi_{j+1},\eta_{m+\frac{1}{2}})$ and (5.3) at the point $(\xi_{j+\frac{1}{2}},\eta_{m+\frac{1}{2}})$. Only two ξ-stations $(j,j+1)$ have to be considered at once and the values at the old station ξ_j are denoted by a superbar; thus, for any dependent variable we use the abbreviated notation

$$\phi_m = \phi(\xi_{j+1},\eta_m) \quad \text{and} \quad \overline{\phi}_m = \phi(\xi_j,\eta_m).$$

Writing the approximations to (5.1), (5.2) and (5.3) for $m = 1,2,\ldots,M-1$, we obtain

$$G_{m+1} - G_m - (h_m/2)(w_{m+1}+w_m) = 0, \tag{5.6}$$

$$w_{m+1} - w_m - (h_m/2)(z_{m+1}+z_m) = 0, \tag{5.7}$$

and

$$A_m(G_{m+1}+G_m) + B_m(w_{m+1}+w_m) + C_m z_{m+1} + D_m z_m - H_m = 0, \tag{5.8}$$

where

$$A_m = (\tfrac{1}{2} + 2\xi_{j+\frac{1}{2}}/k_j)\,h_m F''_{m+\frac{1}{2}}, \quad B_m = -(2F'_{m+\frac{1}{2}}/k_j + i)\,h_m \xi_{j+\frac{1}{2}},$$
$$C_m = 1 + \tfrac{1}{2}h_m F_{m+\frac{1}{2}}, \quad D_m = -1 + \tfrac{1}{2}h_m F_{m+\frac{1}{2}},$$

and

$$H_m = (1 - \tfrac{1}{2}h_m F_{m+\frac{1}{2}})\,\overline{z}_m - (1 + \tfrac{1}{2}h_m F_{m+\frac{1}{2}})\,\overline{z}_{m+1} + (i - 2F'_{m+\frac{1}{2}}/k_j)$$
$$\times h_m \xi_{j+\frac{1}{2}}(\overline{w}_m + \overline{w}_{m+1}) - (\tfrac{1}{2} - 2\xi_{j+\frac{1}{2}}/k_j)\,h_m F''_{m+\frac{1}{2}}(\overline{G}_{m+1} + \overline{G}_m) - 4ih_m\xi_{j+\frac{1}{2}}.$$

In obtaining (5.8) average values, with second-order accuracy, were used in (5.3), e.g.

$$z(\xi_{j+\frac{1}{2}},\eta_{m+\frac{1}{2}}) = \tfrac{1}{4}(z_m + z_{m+1} + \overline{z}_m + \overline{z}_{m+1}),$$

and

$$w_\xi(\xi_{j+\frac{1}{2}},\eta_{m+\frac{1}{2}}) = (w_{m+1} - \overline{w}_{m+1} + w_m - \overline{w}_m)/2k_j.$$

The initial condition requires

$$G_m = \tfrac{1}{2}(\eta_m F'_m + F_m) \quad \text{for} \quad \xi = 0 = \xi_1, \quad m = 1, 2, \ldots, M. \tag{5.9}$$

The boundary conditions will be satisfied if

$$G_1 = 0 = w_1 \quad \text{for} \quad \xi \geqslant 0, \tag{5.10}$$

and

$$w_M = 1 \quad \text{for} \quad \xi \geqslant 0.\dagger \tag{5.11}$$

With a profile given at station ξ_j, (5.6)–(5.8) and (5.10) and (5.11) are $3M$ linear algebraic equations in $3M$ unknowns. Following Keller & Cebeci, this system of equations could be written in a block-matrix form with a coefficient matrix which is tridiagonal. This form is useful for discussing the conditions under which solutions exist and a standard block-tridiagonal factorization procedure might be used to solve this system (see Isaacson & Keller 1966, p. 58). An alternative method is proposed here which is faster and more efficient.

To use our method, we eliminate z_m from (5.6)–(5.8) by the following steps. (i) Solve (5.7) for z_{m+1}, and use it to eliminate z_{m+1} from (5.8). Denote the resulting equation by (A). (ii) Rewrite (5.7) and (5.8) by replacing m with $m-1$, and eliminate z_{m-1} to obtain equation (B). (iii) Combine (A) and (B) to eliminate z_m. We thus obtain the equation

$$A'_m G_{m+1} + B'_m G_m + C'_m G_{m-1} + D'_m w_{m+1} + E'_m w_m + K'_m w_{m-1} - H'_m = 0 \quad \text{for} \quad m = 2, 3, \ldots, M-1, \tag{5.12}$$

where

$$A'_m = 2A_m, \quad B'_m = 2(A_m + A_{m-1}), \quad C'_m = 2A_{m-1}, \quad D'_m = 2(B_m + 2C_m/h_m),$$
$$E'_m = 2(B_m + B_{m-1} + 2D_{m-1}/h_{m-1} - 2C_m/h_m),$$
$$K'_m = 2(B_{m-1} - 2D_{m-1}/h_{m-1}), \quad H'_m = 2(H_m + H_{m-1}).$$

The above equations have been simplified using the result $C_m - D_m = 2$. Considering (5.6), (5.10), (5.11) and (5.12), we now have $2M$ equations and unknowns, and a solution may be found using the algorithm

$$w_{m+1} = \alpha_{m+1} + \beta_{m+1} w_m + \gamma_{m+1} G_m \quad (m = 1, 2, \ldots, M-1), \tag{5.13}$$

combined with (5.6) written in the form

$$G_{m+1} = G_m + (\tfrac{1}{2}h_m)(w_{m+1} + w_m) \quad (m = 1, 2, \ldots, M-1). \tag{5.14}$$

Here,

$$\alpha_m = \{\alpha_{m+1}(D'_m + \tfrac{1}{2}h_m A'_m) - H'_m\}\mathscr{D}^{-1} \quad (m = 2, 3, \ldots, M-1), \tag{5.15}$$

$$\beta_m = \{K'_m + (\tfrac{1}{2}h_{m-1})[A'_m + B'_m + \gamma_{m+1}(D'_m + \tfrac{1}{2}h_m A'_m)]\}\mathscr{D}^{-1} \quad (m = 2, 3, \ldots, M-1), \tag{5.16}$$

$$\gamma_m = \{A'_m + B'_m + C'_m + \gamma_{m+1}(D'_m + \tfrac{1}{2}h_m A'_m)\}\mathscr{D}^{-1} \quad (m = 2, 3, \ldots, M-1), \tag{5.17}$$

and

$$\mathscr{D} = -[(D'_m + \tfrac{1}{2}h_m A'_m)(\beta_{m+1} + \tfrac{1}{2}h_{m-1}\gamma_{m+1}) + E'_m + \tfrac{1}{2}h_m A'_m + (\tfrac{1}{2}h_{m-1}) \times (A'_m + B'_m)] \quad (m = 2, 3, \ldots, M-1). \tag{5.18}$$

† This condition could be replaced with the requirement that a number of points at the top of the profile must satisfy an asymptotic solution valid for large y. Here the boundary-layer thickness is essentially constant as a result of choosing η as independent variable, and (5.11) is satisfactory.

To start the procedure we use (5.11) and (5.13) for $m = M-1$, and choose

$$\beta_M = 0 = \gamma_M \quad \text{and} \quad \alpha_M = 1. \tag{5.19}$$

We then solve (5.15)–(5.17) for the coefficients α_m, β_m, γ_m, while checking at each step that $\mathscr{D} \neq 0$; this will guarantee a non-singular set of equations.† With the coefficients known, w_{m+1} and G_{m+1} may be found from (5.13) and (5.14) by back substitution starting with the values (5.10). Finally, z_1 is determined by eliminating z_2 from (5.7) and (5.8) with $m = 1$, and thereafter using (5.7) with $m = 1, 2, \ldots, M-1$ for $z_m (m > 1)$.

A proof that this method solves the original system, when $\mathscr{D}(m) \neq 0$ ($m = 2, 3, \ldots, M-1$), is easily obtained by mathematical induction and is given in the appendix. It should be noted that after Newton's method is applied to the non-linear finite-difference equations obtained from the non-linear boundary-layer equation (2.2), it is necessary to solve a linear system of equations similar to (5.6)–(5.8) for each iteration and the same algorithm can be used.

This system of equations was programmed, using double-precision complex arithmetic, for an IBM 360/50 computer. Two extensive runs were made, one with fixed $k_j = 0{\cdot}1$ and $h_m = 0{\cdot}04\,(0 \leqslant \eta < 1{\cdot}6)$, $0{\cdot}08\,(1{\cdot}6 \leqslant \eta < 3{\cdot}6)$, $0{\cdot}10$ $(3{\cdot}6 \leqslant \eta < 6{\cdot}6)$, and the other using half these values. The profiles contained 96 and 191 points respectively and the shorter run took about 6 min to reach $x = 20$. Richardson extrapolation was used to improve the accuracy from $O(h^2 + k^2)$ to $O(h^4 + k^4)$, where $h \equiv \max_m h_m$ and $k \equiv \max_j k_j$. It was found that the cruder run almost always gave 3 significant figures of accuracy provided the magnitude of the computed numbers exceeded 0·01, the nominal accuracy.

6. Discussion of results

The real and imaginary parts of G_η, which are the perturbations to the x component of velocity (see (2.14) and (2.16)), are shown in figures 2 and 3 for $x = 0{\cdot}0$, $0{\cdot}5$, $1{\cdot}5$, $2{\cdot}5$, $4{\cdot}0$. The dashed curves in figure 3 correspond to the composite asymptotic solutions given by (3.37), and, for all practical purposes, the asymptotic results may be assumed to exist at this station, since the maximum pointwise difference in the velocity profiles is less than 3 %. Note that the ordinate in these figures is η, and, when expressed in this way, the asymptotic profiles far downstream will not be independent of x.

The real and imaginary parts of the skin friction, $\tau_w = G_{\eta\eta}(x, 0)$, are displayed in figure 4, along with the asymptotic results for small and large x; the remarkable accuracy of the asymptotic results should be observed. The magnitude and phase of the skin friction, along with the asymptotic results for large x, are shown in figure 5. The phase has a local maximum at $x \approx 3{\cdot}25$, and the faint oscillations of the numerical curve, causing it to cross the asymptotic curve, are due to the exponentially small oscillatory eigenfunctions.

The magnitude and phase of the reduced volumetric flux, defined by (3.39), are shown in figure 6 with the asymptotic results for large x. Note that near $x = 1{\cdot}5$

† $\mathscr{D}$ may also vanish as a result of not allowing for pivoting during the inversion procedure.

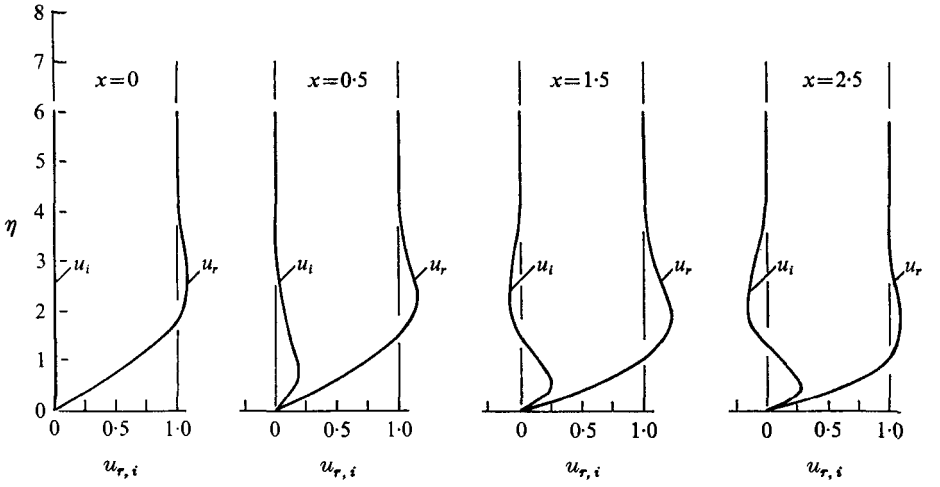

FIGURE 2. Real and imaginary parts of $G_\eta(x,\eta) = u_r + iu_i$ *vs.* η at $x = 0, 0{\cdot}5, 1{\cdot}5, 2{\cdot}5$.

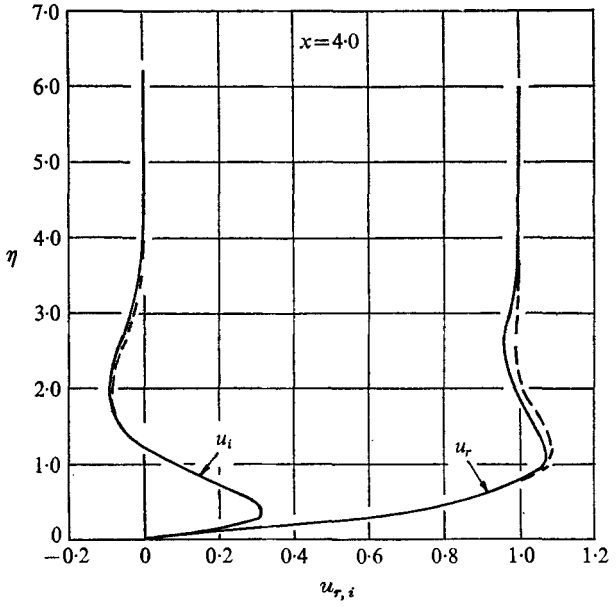

FIGURE 3. A comparison of the real and imaginary parts of $G_\eta(x,\eta) = u_r + iu_i$ from the numerical integration (———) with the asymptotic solution (3·37) (– – – –) at $x = 4{\cdot}0$.

the magnitude of the *volumetric flux* has a local maximum; a glance at the real part of the velocity profile (see figure 2) shows it to be quite full compared to the others. Here the oscillations of the numerical results about the asymptotic curves are quite prominent, and this is the most surprising result of this study. We attribute this behaviour to the eigenfunctions discussed in §4, which oscillate with exponentially decreasing amplitude, and account for different initial conditions upstream.

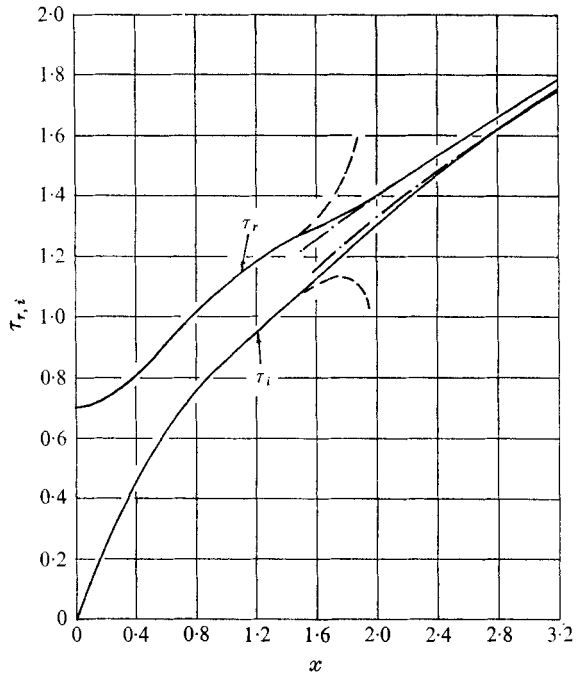

FIGURE 4. Real and imaginary parts of $G_{\eta\eta}(x, 0) = \tau_r + i\tau_i$ *vs.* x. ———, from numerical integration; – – – –, from asymptotic solution about the leading edge (3.1); —·—·—·—, from asymptotic solution for large x (3.38).

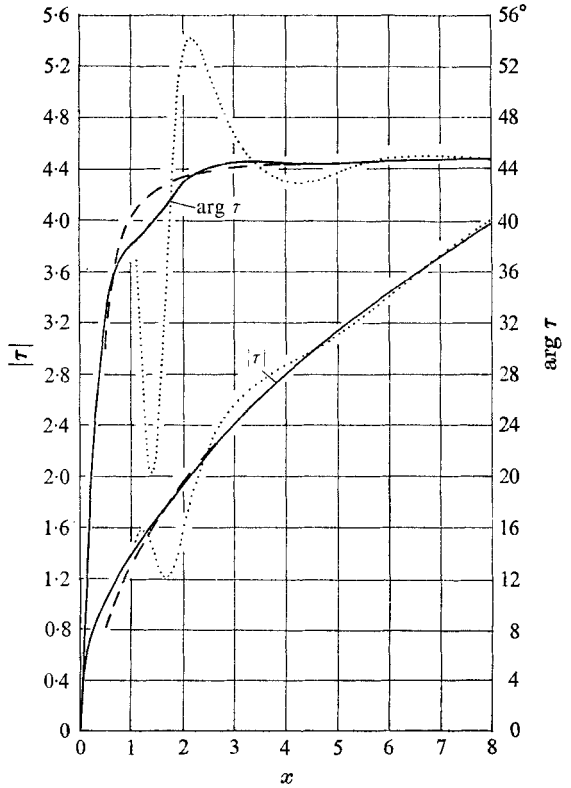

FIGURE 5. Magnitude and argument of $G_{\eta\eta}(x, 0)$ *vs.* x. ———, from numerical integration; – – – – – –, from asymptotic solution for large x (3.38); ....., from different initial conditions at $x = 1{\cdot}0$.

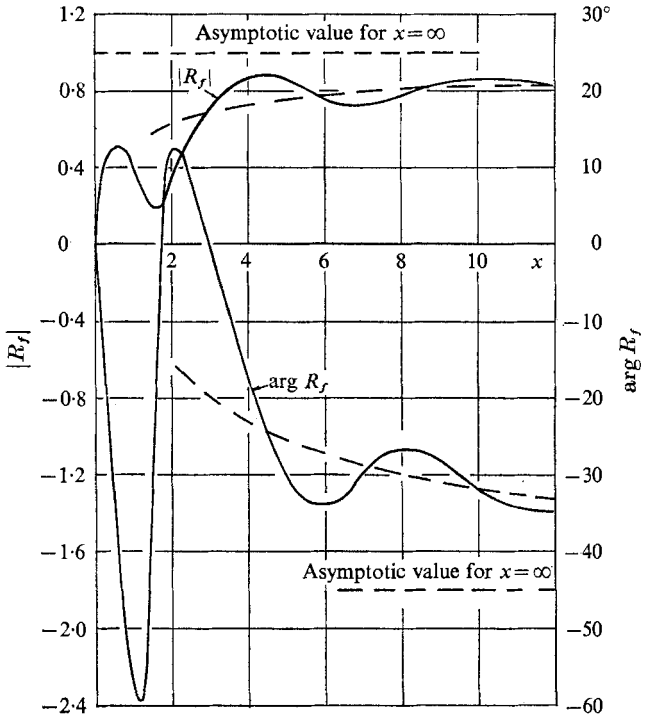

FIGURE 6. Magnitude and argument of the reduced mass flux R_f *vs.* x (3.39). ———, from numerical integration; – – – – –, from asymptotic solution for large x (3.39).

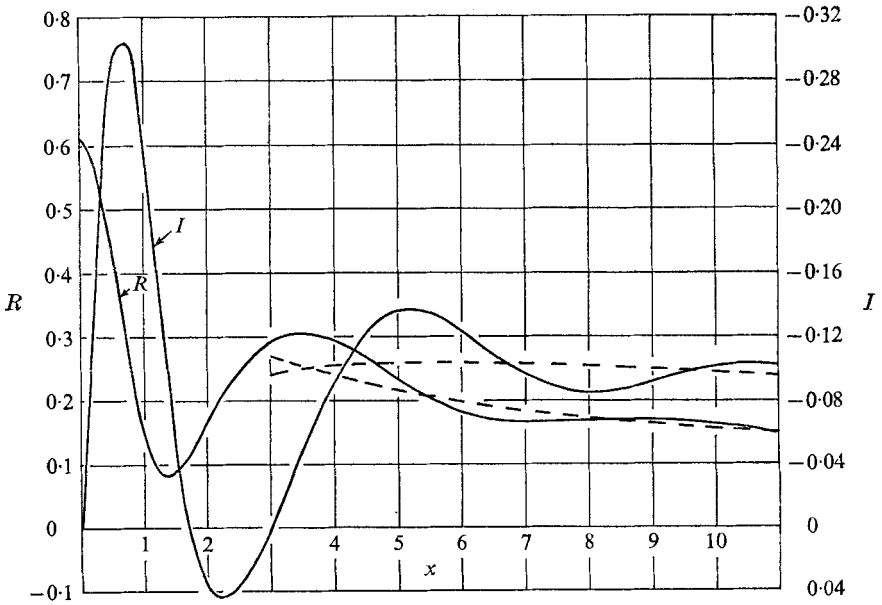

FIGURE 7. Real and imaginary parts of $\lim_{\eta\to\infty}[\eta - G(x,\eta)] = R(x) + iI(x)$ *vs.* x (6.1). ———, from numerical integration; – – – – – – from asymptotic solution (3.39).

To provide evidence supporting this conclusion, consider the real and imaginary parts of

$$R+iI = (2x)^{-\frac{1}{2}} R_f = \int_0^\infty (1-G_\eta)\, d\eta = \lim_{\eta\to\infty} [\eta - G(x,\eta)], \tag{6.1}$$

which are shown in figure 7, along with the asymptotic results for large x. To study the oscillations in detail, we subtract the predicted asymptotic values for large x (3.39), and display the differences $\Delta R + i\Delta I$ in figure 8. It should be noted that the error is $O(x^{-3})$ owing to the neglected terms in (3.39). For large x, the results may also be unreliable because the differences are smaller than the accuracy of

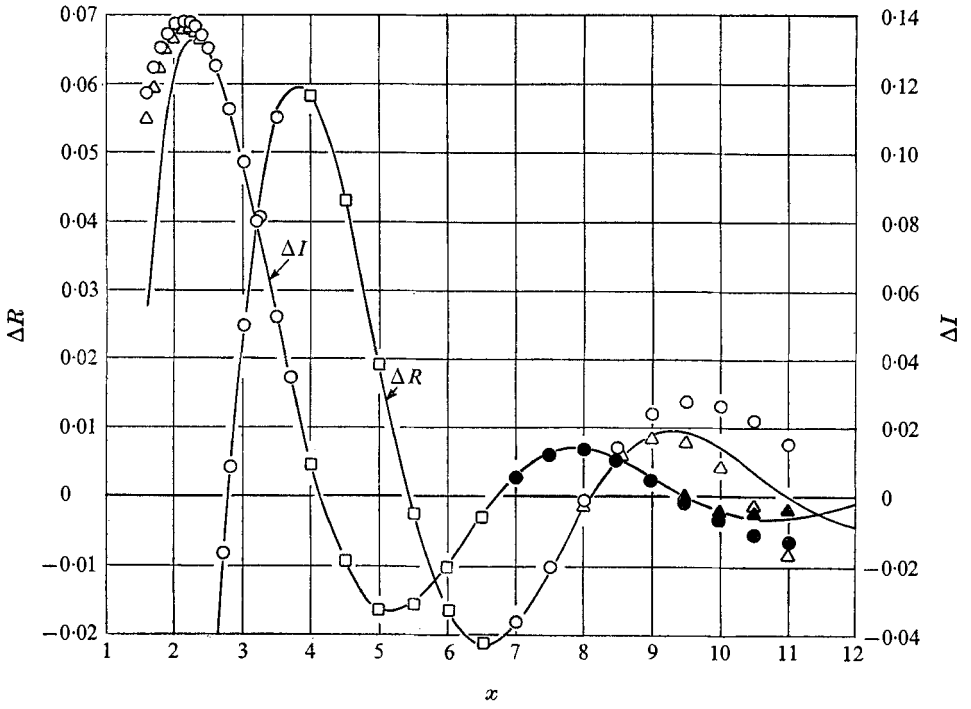

FIGURE 8. The difference, $\Delta R(x) + i\Delta I(x)$, between the numerical and asymptotic values for $x \to \infty$ of $R(x) + iI(x)$ *vs.* x. □, data points used to fit a linear combination of the second, third and fourth eigenfunctions to the numerical results; ○, predicted values from the linear combination of these eigenfunctions; △, predicted values from a linear combination which also includes the fifth eigenfunction. The extra data points used in this case were at $x = 7{\cdot}0$ and $7{\cdot}5$. ●, predictions of the curve ΔI.

the numerical method. We will assume the results are meaningful for $x \in [3, 10]$. Using an approximation containing the second, third, and fourth eigenfunctions, with two unknown constants per eigenfunction (which represent the magnitude and phase), we numerically fitted the approximation at the six x points denoted by squares in figure 8. The points specified by circles represent values predicted by this approximation, and the points denoted by triangles are the predictions of an approximation including the fifth eigenfunction. The additional points taken in the fit for the last case are the next two similarly spaced points at larger x

values. Although the agreement is convincing, we had hoped to predict the real part from the imaginary part (and vice versa), but this was unsuccessful.

The link between the initial conditions and the exponentially small eigenfunctions was provided by the following numerical experiment, for which there is a laboratory analogue that will be discussed below. The integration was started in the usual way, but, at $x = \xi = 1{\cdot}0$, the real part of G_η was increased by 1·0 for $1{\cdot}6 \leqslant \eta \leqslant 4{\cdot}8$ with all other quantities remaining fixed. Two additional steps

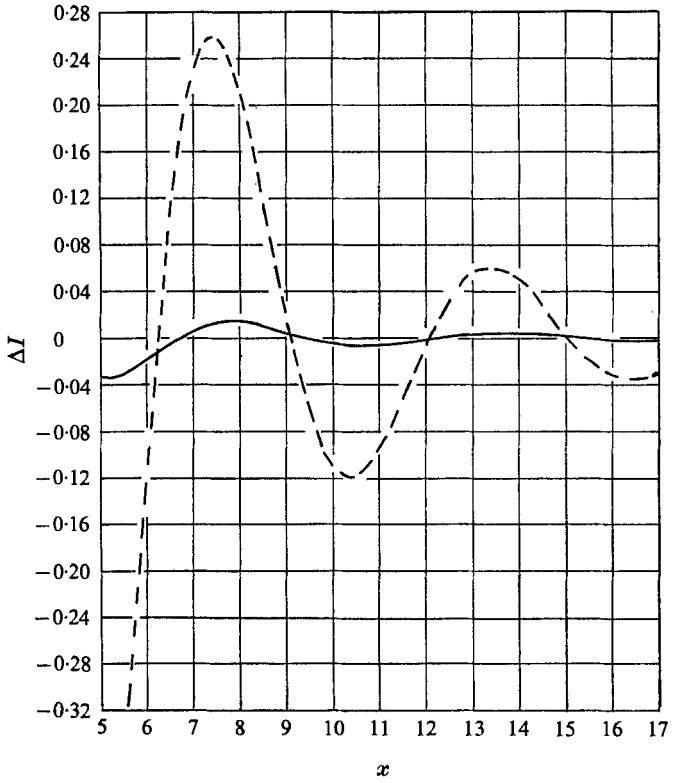

FIGURE 9. A comparison of ΔI computed from initial conditions at $x = 1{\cdot}0$ (– – – –) with the ΔI displayed in figure 8 (———).

in x were taken, with step size Δx, and the resulting sets of data at $x = 1 + \Delta x$ and $1 + 2\Delta x$ were averaged to yield a second-order-accurate solution at the point $x = 1 + \frac{3}{2}\Delta x$. The averaging eliminates spurious numerical oscillations which arise from an inconsistent profile at $x = 1{\cdot}0$.† In any case, since (2.17) is parabolic, the solution may be started at any x with an arbitrary profile,‡ and we choose the starting profile at $x = 1 + \frac{3}{2}\Delta x$, since it is consistent and quite smooth.

The skin friction results from this integration are shown in figure 5 as the dotted curve; the excitation of the exponentially small oscillatory eigenfunctions is

† By a consistent profile we mean that, if $w = G_\eta$ is given along a line $x =$ constant, G and z are determined on that line from (5.1) and (5.2).

‡ The point $x \equiv 0$ is a singular point of (2.17) and to avoid singular solutions (see the discussion following (3.4)), an initial profile at $x \equiv 0$ must satisfy (2.20).

apparent in both the magnitude and phase. This situation could be realized experimentally by injecting some of the free-stream fluid into the boundary layer over the range of η specified above; it would probably not be too difficult to verify the dramatic phase shifts predicted in the range $1 \leqslant x \leqslant 5$.

In figure 9, we have displayed ΔI from the above computation as the dashed curve, with the curve ΔI from figure 8 shown solid. The differences between the curves again indicate that the exponentially small eigenfunctions may be important in determining the way in which the asymptotic state is approached.

More extensive numerical calculations are under way when ϵ is moderately large (of $O(0{\cdot}5)$), when the linearization procedure (2.16) would not be valid. In these cases the non-linear boundary-layer equations must be solved, and extensive regions of backflow are expected. A comparison between numerical results obtained here from the linear theory and those obtained from the non-linear equations indicates the linear theory is quite accurate (with maximum error in the skin friction of 3 %) for $\epsilon \leqslant 0{\cdot}1$.

This research was supported by the U.S. Army Research Office, Durham, under grant DA-ARO-D-31-124-71-G68. An abstract of the paper was presented at the International Union for Theoretical and Applied Mechanics Symposium on Unsteady Boundary Layers at Laval University, Quebec, Canada (May 1971).

Appendix. Validity of the algorithm (5.13)

To establish (5.13), it must be shown that the coefficients α_m, β_m, and γ_m can be determined recursively. Once they are known, w_m, G_m, and z_m can be found by the method outlined below (5.19).

Write (5.6) and (5.12) with $m = N$, and (5.6) with $m = N-1$, i.e.

$$G_{N+1} - G_N - (\tfrac{1}{2}h_N)(w_{N+1} + w_N) = 0 \quad (N = 1, 2, \ldots, M-1),$$

$$A'_N G_{N+1} + B'_N G_N + C'_N G_{N-1} + D'_N w_{N+1} + E'_N w_N + K'_N w_{N-1} - H'_N = 0 \quad (N = 2, 3, \ldots, M-1),$$

$$G_N - G_{N-1} - (\tfrac{1}{2}h_{N-1})(w_N + w_{N-1}) = 0 \quad (N = 2, 3, \ldots, M).$$

Mathematical induction will be used, and we note that the initial values (5.11) and (5.19) satisfy (5.13) with $m = M-1$. Assume (5.13) is true for $m = M-2$, $M-3, \ldots, N$; for induction it must be established for $m = N-1$. For $m = N$, (5.13) can be written

$$\gamma_{N+1} G_N - w_{N+1} + \beta_{N+1} w_N + \alpha_{N+1} = 0 \quad (N = 1, 2, \ldots, M-1).$$

For a fixed N ($N = 2, 3, \ldots, M-1$), the above four equations contain 6 unknowns, G_{N+1}, G_N, G_{N-1}, w_{N+1}, w_N, w_{N-1}, and it should be possible to solve for w_N in terms of G_{N-1}, and w_{N-1}. Solving for w_N by Cramer's rule, we find the resulting equation will be of the form (5.13) with $m = N-1$, provided the coefficients α_N, β_N, γ_N are related to α_{N+1}, β_{N+1}, γ_{N+1} by the recursion formulas (5.15)–(5.18); this establishes the result.

No difficulty will be encountered unless the denominator $\mathscr{D}(m)$, given by (5.18), vanishes for some m. In that case, the system of equations may be singular, but it is more likely that a rearrangement of the equations or a different method of solution will avoid this difficulty.

REFERENCES

ABRAMOWITZ, M. & STEGUN, I. A. 1964 *Handbook of Mathematical Functions, with Formulas, Graphs, and Mathematical Tables.* Washington, D.C.: U.S. Government Printing Office.

ACKERBERG, R. C. 1968 Boundary-layer flow on a vertical plate. *Phys. Fluids*, **11**, 1278–1291.

ACKERBERG, R. C. 1970 Boundary-layer separation at a free streamline. Part 1. *J. Fluid Mech.* **44**, 211–225.

COLE, J. D. 1968 *Perturbation Methods in Applied Mathematics.* Waltham, Mass.: Blaisdell.

GOLDSTEIN, S. 1930 Concerning some solutions of the boundary-layer equations in hydrodynamics. *Proc. Camb. Phil. Soc.* **26**, 1–30.

ISAACSON, E. & KELLER, H. B. 1966 *Analysis of Numerical Methods.* Wiley.

KELLER, H. B. & CEBECI, T. 1971 Accurate numerical methods for boundary layer flows. Part 1. Two-dimensional laminar flows. *Proc. Int. Conf. on Numerical Methods in Fluid Dynamics.* (Published as *Lecture Notes in Physics.* Springer.)

LAM, S. H. & ROTT, N. 1960 Theory of linearized time-dependent boundary layers. *Cornell University GSAE Rep. AFOSR* TN-60-1100.

LIBBY, P. A. & FOX, H. 1963 Some perturbation solutions in laminar boundary-layer theory. Part 1. *J. Fluid Mech.* **17**, 433–449.

LIGHTHILL, M. J. 1954 The response of laminar skin friction and heat transfer to fluctuations in the stream velocity. *Proc. Roy. Soc.* A **224**, 1–23.

LIN, C. C. 1956 Motion in the boundary layer with a rapidly oscillating external flow. *Proc. 9th Int. Congr. Appl. Mech., Brussels*, **4**, 155–167.

ROTT, N. & ROSENZWEIG, M. L. 1960 On the response of the laminar boundary layer to small fluctuations of the free-stream velocity. *J. Aero. Sci.* **27**, 741–747.